

Effects of Magnetic Fields on Neutrino-dominated Accretion Model for Gamma-ray Bursts

Yi Xie*, Chang-Yin Huang and Wei-Hua Lei

Department of Physics, Huazhong University of Science and Technology, Wuhan 430074,
China

Abstract Many models of gamma-ray bursts suggest a common central engine: a black hole of several solar masses accreting matter from a disk at an accretion rate from 0.01 to $10 M_{\odot} s^{-1}$. The inner region of the disk is cooled by neutrino emission and large amounts of its binding energy were liberated, which could trigger the fireball. We improve the neutrino-dominated accreting flows by considering the effects of the magnetic fields, and find that more than half of the liberating energy can be extracted directly by the large-scale magnetic fields on the disk. And it turns out that the temperature of the disk is a bit lower than the neutrino-dominated accreting flows without magnetic field. Therefore, The outflows are magnetically-dominated rather than neutrino dominated. In our model, neutrino mechanism can fuel some GRBs (not the brightest ones), but cannot fuel X-ray flares. However, the magnetic processes (both BZ and electromagnetic luminosity from a disk) are viable mechanisms for most of GRBs and the following X-ray flares.

Key words: magnetic fields—accretion, accretion disks—neutrinos—gamma rays: bursts

1 INTRODUCTION

Gamma-ray bursts (GRBs) are flashes of gamma-rays occurring at cosmological distances, being the most powerful explosions since the Big Bang. They are generally divided into two classes (Kouveliotou et al.1993): short-duration ($T_{90} < 2s$) hard-spectrum GRBs (SGRBs) and long-duration ($T_{90} > 2s$) soft-spectrum GRBs (LGRBs), which have different progenitors. LGRBs root in core collapses of massive, rapidly rotating stars (Woosley 1993, Paczynski 1998, Hjorth et al 2003, Stanek et al 2003), and supernovae have been observed coincidentally in some LGRBs (Galama et al 1998; Stanek et al 2003; Hjorth 2003). In contrast to LGRBs, SGRBs may arise from coalescence of neutron stars or black hole binary systems due to damping of gravitational radiation (e.g. Eichler et al. 1989, Narayan, Paczynski & Piran 1992, Fryer &

* E-mail: sourcexieyi@gmail.com

Woosley 1998), and they are probably associated with elliptical galaxies (Gehrels et al. 2005; Bloom et al 2006; Barthelmy et al. 2005; Berger et al 2005). It is believed that the two processes give rise to a black hole of several solar masses with a magnetized disk or a torus around it (Meszaros & Rees 1997b). And many central engine models of GRBs based on this scenario (exception models, for instance, magnetizedrotating neutron stars, see e.g. Usov 1992).

Some authors have studied the accretion model for GRBs by assuming steady-state accretion (e.g. Papham, Woosley & Fryer 1999, hereafter PWF; Narayan, Piran & Kumar 2001, hereafter NPK; Di Matteo, Perna & Narayan 2002, hereafter DPN). Their studies show that at the extremely high accretion rate (0.01 to $10 M_{\odot} s^{-1}$) needed to power GRBs, the disk cannot be cooled efficiently as the gas photon opacities are very high, and a large fraction of its energy is advection dominated. However, inner region of the disk becomes hot and dense enough to cool via neutrino emission, and this accretion mode is referred to as neutrino-dominated accretion flows (NDAFs). The neutrinos can liberate large amounts of binding energy via the $\nu\bar{\nu} \rightarrow e^+e^-$ processes in regions of low baryon density and then trigger the fireball.

However, the model with "neutrino-driven outflow" alone cannot be a candidate of some GRBs central engine. For instance, numerical simulations by Shibata et al. (2006) suggest that the collapse of hypermassive neutron-star triggered by gravitational wave cannot be a candidate for the central engine of SGRBs, however, it becomes powerful enough to produce the fireball after taking the magnetic braking and MRI into account. On the other hand, researches show that the magnetic fields can be magnified up to $10^{15} \sim 10^{16} G$ by virtue of magnetorotational instability (MRI, Balbus & Hawley 1991) or dynamo processes (Pudritz & Fahlman 1982 and references therein) in the inner region of the disk. So, the existence of strong magnetic fields should be considered. Both PWF and DPN compared the luminosity of neutrino emission and Poynting flux, and indicated that MHD processes are viable mechanisms for powering GRBs, but they did not include magnetic fields in their disk conditions.

In this paper, we intend to improve the NDAF model by considering the effects of magnetic braking and magnetic viscosity. The equation of angular momentum of a standard disk is replaced by the equation of a magnetized disk in which the viscosity caused by magnetic braking and magnetic viscosity only. Meanwhile, we deduce the rotational energy extracted by large-scale fields in the disk from the thermal energy produced by viscous dissipation, and the magnetic pressure is considered in equation of state else. It turns out that the inner region of the disk is magnetically dominated. Magnetized accretion models within the GRB context have been also discussed in several other papers in which detailed numerical simulations are performed. For example, Proga et al. (2003) studied a MHD collapsar accretion model and suggested that MHD effects alone can launch a GRB jet, which is Poynting flux dominated. Mizuno et al. (2004a; 2004b) drew similar conclusions using a GR-MHD code. These results agree with our conclusion in this paper.

This paper is organized as follows. In Section 2 we outline the theory of a magnetized accretion disk. In Section 3 we introduce the basic assumptions and equations of our model. In Section 4 we show the numerical results of our model, and finally, In Section 5 we summarize main results of our model and some defects are discussed.

2 DESCRIPTION OF A MAGNETIZED ACCRETION DISK

It is widely known that the magnetic fields on the disk can greatly affect angular momentum transfer and hence the accretion rate via a variety of modes. In this paper we only consider two basic mechanisms: the first one is magnetic viscosity, the weak magnetic fields creates MRI in which turbulence dominates the angular momentum transfer (Balbus & Hawley 1991). The second is the magnetic braking, the large scale magnetic field extracts rotational energy of disk due to the shear force of differential rotation (Blandford 1976; Blandford & Payne 1982;

Livio et al 1999). We assume that the accretion process is governed by these two mechanisms completely. The main points of the magnetized accretion disk model (in which the magnetic braking and magnetic viscosity are considered only for angular momentum transfer) given by Lee et al. (2000) are outlined as follow.

According to Torkelsson et al. (1996) the magnetic viscosity ν^{mag} is defined as

$$B_\phi B_r / 4\pi = -\nu^{mag} (rd\Omega_{disk}/dr) \rho, \quad (1)$$

where B_ϕ and B_r are respectively the azimuthal and radial components, Ω_{disk} is angular velocity and ρ is the density of the disk matter. The magnetic viscosity ν^{mag} can be parameterized as (Shakura & Sunyaev 1973; Pringle 1981)

$$\nu^{mag} = \alpha^{mag} c_s H, \quad (2)$$

where c_s is the sound velocity of the disk ($c_s = (P_{disk}/\rho)^{1/2}$, in which P_{disk} is the disk pressure) and H is the half-thickness of the disk. Invoking hydrostatic equilibrium perpendicular to the disk plane, we have $H = c_s/\Omega_{disk}$ and

$$\nu^{mag} = \alpha^{mag} c_s^2 / \Omega_{disk}. \quad (3)$$

For a Keplerian orbit we have $\Omega_{disk} \sim \Omega_K = (GM/r^3)^{1/2}$, and Eq. (1) can be written as

$$B_\phi B_r / 4\pi = \frac{3}{2} \alpha^{mag} P_{disk}. \quad (4)$$

The accretion rate is generally determined by magnetic braking for $H \ll r$ (Lee, Wijers & Brown 2000), the angular momentum balance equation can be written as

$$\dot{M} = 2r B_\phi B_Z / \Omega_{disk}. \quad (5)$$

The axisymmetric solution (Blandford 1976) is

$$B_\phi = 2r \Omega_{disk} B_Z / c. \quad (6)$$

A roughly steady state will be reached when the grown rate of B_ϕ generated by differential rotation from radial field equals to its loss rate by buoyancy, then the magnitude of B_ϕ can be estimated as (Katz 1997)

$$B_\phi \approx \left[\frac{3}{2} B_r \Omega_{disk} H \right]^{1/2} (4\pi\rho)^{1/4}. \quad (7)$$

By using Eqs. (4), (6) and (7) we have

$$B_Z = \frac{c}{2} \left(\frac{\pi r P_{disk}}{GM} \right)^{1/2} (9\alpha^{mag})^{1/3}, \quad (8)$$

and

$$B_\phi = (\pi P_{disk})^{1/2} (9\alpha^{mag})^{1/3}. \quad (9)$$

The vertical component and azimuthal component of field can be estimated by using Eqs. (8) and (9), and for a given α^{mag} , only depending on the gas pressure.

Combining Eqs. (6) and (8) with Eq. (5) we have (see also Lee, Wijers & Brown 2000)

$$\dot{M} = 4r^2 B_Z^2 / c. \quad (10)$$

Since \dot{M} is independent of r in steady-state accretion, we can infer that $B_Z \propto 1/r$.

3 BASIC ASSUMPTIONS AND EQUATIONS OF MODEL

The basic physical conditions in disk models for GRBs can be derived by virtue of steady-state conditions (PWF, NPK, DPN). Base on these studies, we consider the effects of magnetic field in inner regions of disks in the frame of hydrodynamics. The basic equations consist of equation of state and the conservation equations of energy and angular momentum in a magnetized accretion disk, which are described as follows.

In equation of state we include the contributions from radiation pressure, gas pressure, degeneracy pressure and magnetic pressure,

$$P = \frac{11}{12}aT^4 + \frac{\rho kT}{m_p} + \frac{2\pi hc}{3} \left(\frac{3}{8\pi m_p} \right)^{4/3} \left(\frac{\rho}{\mu_e} \right)^{4/3} + \frac{B^2}{8\pi}, \quad (11)$$

where a is the radiation constant, T is the disk temperature, and the factor $\frac{11}{12}$ includes the contribution of relativistic electron-positron pairs. In degeneracy term, μ_e is the mass per electron, and it is taken as 2 by assuming equal number of protons and neutrons. For the magnetic pressure we only consider poloidal component in calculation, provided that it is not much less than the toroidal component.

The conservation of mass is written by NPK and DPN as follows,

$$\dot{M} = 4\pi r v_r \rho H \approx 6\pi \rho \nu H, \quad (12)$$

where v_r is the radial velocity and $v_r = 3\nu/2r$. Different from NPK and DPN, we replace the Eq. (12) by Eq. (10), which includes the effects of magnetic braking and magnetic viscosity.

In energy equation, the viscous heating equals neutrino radiative loss plus advective loss and the fraction of rotational energy extracted by large-scale magnetic fields

$$\frac{3GM\dot{M}}{8\pi r^3} = (q_{\nu\bar{\nu}}^- + q_{eN}^-) H + q_{adv} + Q_B^-, \quad (13)$$

in which $q_{\nu\bar{\nu}}^-$ is cooling via pair annihilation and we take it as the approximation of Itoh et al. (1989; 1990): $q_{\nu\bar{\nu}}^- \simeq 5 \times 10^{33} T_{11}^9 \text{ergscm}^{-3} \text{s}^{-1}$ (in which $X_n = X/10^n$ is used). The q_{eN}^- represents the cooling via pair capture on nuclei, and can be estimated as $q_{eN}^- \simeq 9 \times 10^{33} \rho_{10} T_{11}^6 \text{ergscm}^{-3} \text{s}^{-1}$. And q_{adv} is the advective cooling rate, we approximate it by (see eg., Narayan & Yi 1994; Abramowicz et al.1995)

$$q_{adv} = \Sigma \nu T \frac{ds}{dr} \simeq \xi \nu \frac{H}{r} T \left(\frac{11}{3} a T^3 + \frac{3}{2} \frac{\rho k T}{m_p} \frac{1 + X_{nuc}}{4} \right), \quad (14)$$

in which s is specific entropy, X_{nuc} is the mass fraction of free nucleons, $\xi \propto -d \ln s / d \ln r$ is assumed to be equal to 1 as in DPN. And finally, Q_B^- represents the energy extracted by magnetic field (see, Lee, Wijers & Brown 2000)

$$Q_B^- = \frac{dP^{mag}}{dS} = \frac{B_Z^2 r^2}{\pi c} \left(\frac{GM}{r^3} \right) = \frac{GM\dot{M}}{4\pi r^3}, \quad (15)$$

where $dS = 2\pi r dr$. Comparing Eq.(15) with Eq.(13), we find that two thirds of energy of viscous heating was substituted by the field extracting, therefore, it is magnetically dominated in the inner regions of disks.

Eqs. (8), (10), (11) and (13) contain four independent unknowns P , ρ , T and B_Z as functions of r and compose a complete set of equations which can be numerically solved with given M , α (for simplicity, we omit the superscript 'mag') and \dot{M} . In the following calculations we fix $M = 3M_\odot$ (the corresponding Schwarzschild radius R_s is $2GM/c^2 = 8.85 \times 10^5 \text{cm}$), $\alpha = 0.1$.

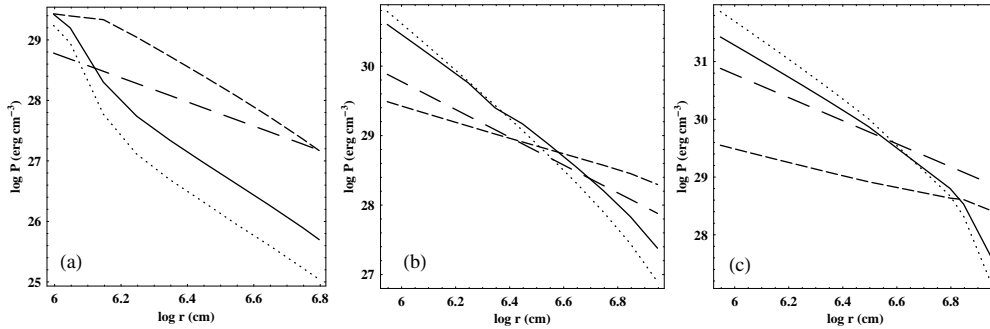


Fig. 1 Pressure components profiles for three values of the accretion rate: (a) $\dot{m} = 0.1$, (b) $\dot{m} = 1$, and (c) $\dot{m} = 10$. The gas pressure is shown by the solid line, degeneracy pressure by dotted line, radiation pressure by dashed line, and magnetic pressure by long-dashed line.

4 NUMERICAL RESULTS

4.1 Gas Profiles

We show the numerical solutions of the full equations in this section, and the software of "Mathematica" is used for the numerical algorithm of Newton iteration method. The pressure components profiles are shown in Figure 1, and the solutions for three values of the accretion rate $\dot{m} = 0.1, 1$, and 10 (\dot{m} is defined as $\dot{m} = \dot{M}/M_{\odot} s^{-1}$) are shown in (a), (b) and (c) respectively. The gas pressure, degeneracy pressure, radiation pressure, and magnetic pressure are shown by the solid line, dotted line, dashed line, and long-dashed line, respectively. From Figure 1, we obtain the following results:

(i) From (a) we can see that, the flows is radiation pressure dominated in the region of $1R_S \sim 10R_S$ and may be thermally unstable (see 4.3, stability analysis). It is thermally stable in the same region in DPN as it always dominates by gas pressure.

(ii) From (b) and (c) we can see that, the magnetic pressure component is more important at large radii and even overwhelms the gas pressure and degeneracy pressure. So our model is valid only in a narrow region because of the restriction of Eq. (12).

Temperature and density profiles calculated from our model are shown in Figure 2. We show our solutions for three values of the accretion rate, $\dot{m} = 0.1, 1$, and 10 (long dashed, solid, and short-dashed lines, respectively). Comparing with DPN (see DPN, Fig.1), we find that the temperature of disk is a bit lower than NDAFs without considering the effects of magnetic fields, and the density drops much more rapidly with the radius.

4.2 BZ Luminosity, Electromagnetic Luminosity from Disk, and Neutrino Luminosity

It is a common assumption that the magnetic fields will rise up to some fraction, which for instance in DPN, 10% of its equipartition value $B^2/8\pi \sim \rho c_s^2$. For $0.1 < \dot{m} < 10$, the typical values of ρc_s^2 are $10^{30} \sim 10^{32} \text{ erg cm}^{-3}$, implying a field strength of $10^{15} \sim 10^{16} G$. The BZ jet luminosity is then

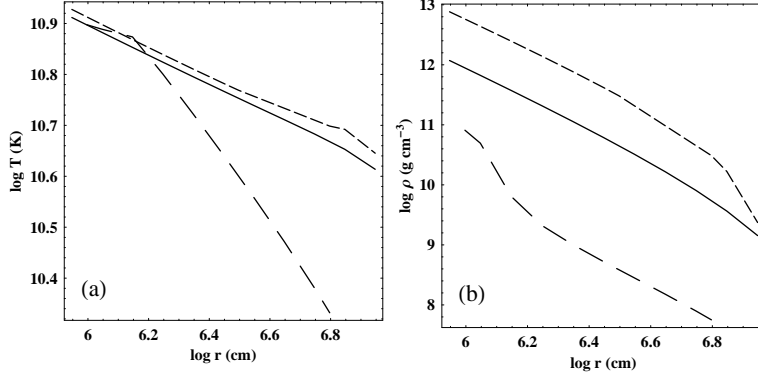


Fig. 2 Temperature and density profiles in (a) and (b) respectively. The profiles are shown for three values of the accretion rate: $\dot{m} = 0.1$ (long dashed lines), $\dot{m} = 1$ (solid lines), and $\dot{m} = 10$ (short dashed lines).

$$L_{BZ} = \frac{B_H^2}{4\pi} \pi c a^2 R_S^2 \simeq 10^{52} a^2 \left(\frac{B_H}{10^{16} G} \right)^2 \left(\frac{M}{3M_\odot} \right)^2 \text{ ergs cm}^{-3}, \quad (16)$$

in which a is the dimensionless black hole spin parameter, B_H is the magnetic field on the horizon.

The electromagnetic power output from a disk is equal to the power of the disk magnetic braking can be calculated as (Livio et al. 1999; Lee et al. 2000)

$$L_d = \frac{B_z^2}{4\pi} \pi r^2 \left(\frac{r \Omega_{disk}}{c} \right) c \approx a^{-2} \left(\frac{B_Z}{B_H} \right)^2 \left(\frac{r}{R_S} \right)^{3/2} L_{BZ}. \quad (17)$$

Consistent with previous work (Merloni & Fabian 2002; DPN), we take approximately,

$$B_Z \sim (H/r) B_H. \quad (18)$$

It is easy to get the strength of poloidal field in the disk and the field on the black hole horizon for a given \dot{m} by using Eqs. (10) and (18) in our model, without the assumption of equipartition value discussed above. And then, the BZ jet luminosity and the electromagnetic power from a disk can be calculated from Eqs. (16) and (17). The neutrino luminosity is given by $L_\nu = \int_{r_{min}}^{r_{min}^{max}} 2\pi q_\nu^- r dr$, in which $q_\nu^- = (q_{\nu\bar{\nu}}^- + q_{eN}^-) H$, $r_{min} = 1R_S$ (for an extreme Kerr black hole), and $r_{min}^{max} = 10R_S$. We estimate the luminosity due to $\nu\bar{\nu}$ annihilation along z-axis above the disk to be the Eq. (21) in DPN. In Figure 3 we show the curves of BZ luminosity L_{BZ} (solid lines), electromagnetic luminosity from a disk L_d (long-dashed line), and neutrino annihilation luminosity $L_{\nu\bar{\nu}}$ (short-dashed line) versus dimensionless accretion rate. From Figure 3, we obtain the following results:

(i) L_d is larger than L_{BZ} for $H/r = 0.2$ (solution of this model), however, both of them are viable mechanisms for central engines of GRBs, and can also fuel the observed X-ray flares in which case the accretion rate of $\dot{m} = 0.01$ is needed.

(ii) The $L_{\nu\bar{\nu}}$ is around $10^{51} \text{ ergs s}^{-1}$ at $\dot{m} = 1$, which is sufficient to power some GRBs, and at the accretion rate of $\dot{m} = 0.01$, it fails to fuel the X-ray flares.

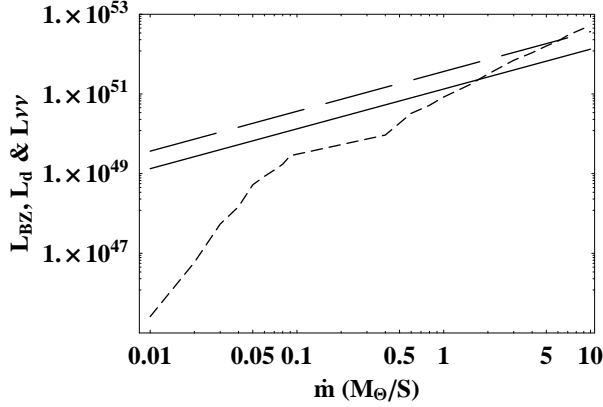


Fig. 3 The solid lines represent the BZ luminosity, and the long-dashed line represent the electromagnetic luminosity from a disk and short-dashed line represents neutrino annihilation luminosity as a function of accretion rate and value of $H/r = 0.2$.

In conclusion, neutrino mechanism can fuel some GRBs (not the brightest ones), but cannot fuel X-ray flares. However, the magnetic processes (both BZ and electromagnetic luminosity from a disk) are viable mechanisms for most of GRBs and the following X-ray flares (this agrees well with discussions of Fan et al. (2005)).

4.3 Stability

Both NPK and DPN discussed the stability properties of their solutions. Since our model considers the effects of magnetic fields and differs considerably with theirs, it is interesting to examine whether the solution is stable.

The general condition for thermal stability is given by (Piran 1978)

$$\left(\frac{d \ln Q^+}{d \ln T} \right)_{|\Sigma} < \left(\frac{d \ln Q^-}{d \ln T} \right)_{|\Sigma}, \quad (19)$$

in which Q^\pm are the integrated (over the height of the disk) heating (+) and cooling (-) rates. The cooling rate $Q^- = q_\nu^- + q_{adv} + Q_B^-$. We show the two curves of Q^- and Q^+ as a function of gas temperature in Figure 4. The radius is fixed at $r = 5R_S$, while the surface density is taken to be $\Sigma = 10^{16} gcm^{-2}$. From Figure 4 we can see that, the flow is unstable while the temperature T is lower than $5 \times 10^{10} K$, because the magnetic fields extract rotational energy from disk is independent with temperature. When $T > 5 \times 10^{10} K$, it turns to stable because $q_{eN}^- \propto T^6$ becomes relatively significant with the temperature increasing. When the disk temperature crosses the critical point of the instability curves, the thermal energy would be released suddenly in a thermal time scales. It is possibly an explanation for the variability time scales of tens of msec in the light curves of the GRBs, and we will give the details in another paper.

Following NPK and DPN we use the condition for viscous stability

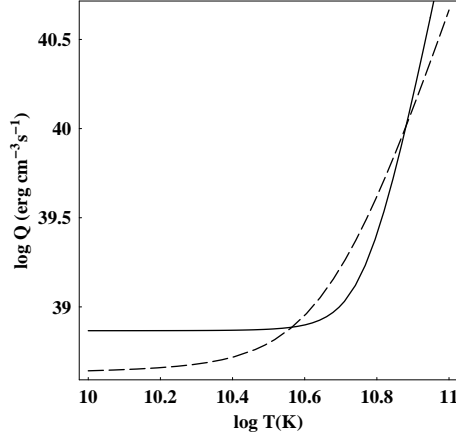


Fig. 4 Thermal stability analysis. Dashed line shows Q^+ and solid line shows Q^- vs. T for $r = 5R_S$ curves, and for $\Sigma = 10^{16} \text{ g cm}^{-2}$. The solution is unstable while $T < 5 \times 10^{10} \text{ K}$, and becomes stable when $T > 5 \times 10^{10} \text{ K}$.

$$\frac{d\dot{M}}{d\Sigma} > 0. \quad (20)$$

In our model, we have $\dot{M} \propto \Sigma$ for the case of gas pressure dominated, $\dot{M} \propto \Sigma^{8/7}$ for degeneracy pressure case, $\dot{M} \propto \Sigma^2$ for radiation pressure case, and we have $\dot{M} \propto B^2 \propto P$ for the magnetic dominated and the surface density $\Sigma \propto P^{1/2} \rho^{1/2}$, meanwhile, considering the magnetic fields decreases as r^{-1} , we have approximately $\rho \propto r^{-3}$, and then $\dot{M} \propto \Sigma$. All of these cases are clearly viscously stable.

Finally, we also consider the gravitational instability. The accretion flow will become gravitational unstable if the Toomre parameter Q_T is less than 1, for a Keplerian orbit, which is given by (Toomre 1964)

$$Q_T = \frac{c_s \kappa}{\pi G \Sigma} = \frac{\Omega_K^2}{\pi G \rho}. \quad (21)$$

We have checked that $Q_T \gg 1$ hence the flow is gravitationally stable in the inner region of the disk. Nevertheless, at large radii the Toomre parameter could be less than 1 as argued by Perna et al. (2006). Actually that was another model for X-ray flares.

5 CONCLUSION AND DISCUSSION

In this paper we modify the NDAFs model as a central engines for GRBs by considering the effects of magnetic braking and magnetic viscosity in the frame of Newtonian dynamics. We found that two thirds of the liberating energy was extracted directly by large-scale magnetic fields on the disk and the temperature of a disk is a bit lower than the NDAFs without magnetic fields. Furthermore, the density of the disk drops faster than NDAFs along the radius. Therefore, the inner region of the flow is magnetically dominated rather than neutrino dominated. However,

the neutrino mechanism can still fuel some GRBs (not the brightest ones), but cannot fuel X-ray flares. However, the magnetic processes (both BZ and electromagnetic luminosity from a disk) are viable mechanisms for most of GRBs and the following X-ray flares.

Our model is formulated invoking Newtonian potential, ignoring the effects of general relativity which may be important in some aspects (Gu et al. 2006) and neutrino opacity. Specially, the main simplification of the analytic approach (this and other analytical works) is the requirement of a steady state, which in reality (e.g. numerical simulations) is not necessarily justified. An example is that with magnetic fields, both numerical simulations (Proga & Begelman, 2003) and some analytical arguments (Proga & Zhang, 2006) suggest that the accretion flow may not always in a steady state. Rather, magnetic fields accumulated near the black hole can form a magnetic barrier that temporarily blocks the accretion flow. This makes some dormant epochs at the central engine. The breaking of the barrier would lead to restarting the central engine, which is required to explain the recent Swift observations of X-ray flares (for a review of Swift results and in particular X-ray flares and their interpretations, see Zhang, 2007). In this paper, the poloidal component of magnetic fields is $B_Z \propto 1/r$, which implies that the magnetic pressure drops much slower than the other components and the calculations indicate that the magnetic fields pressure could be dominant at larger radii. In fact, such over-pressure magnetic fields are the agent to form the magnetic barrier as reported by Proga & Zhang, which is needed to interpret the observed X-ray flares. The unsteady state accretion model and the case of over-pressure magnetic fields will be studied in our future work.

Acknowledgements We would like to thank the referee, whose comments led to a significant improvement of this work. This work is supported by the National Natural Science Foundation of China under grants 10573006.

References

- Abramowicz M. A., Chen X., Kato S., Lasoto J. P., & Regev O., 1995, ApJ, 438, L37
 Balbus, S. A., & Hawley J. F., 1991, ApJ, 376, 214
 Berger et al, 2005, Nature, 438, 988
 Barthelmy S.D. et al. 2005, Nature, 438, 994
 Blandford R.D., 1976, MNRAS, 176, 456
 Blandford R. D., & Payne D. G., 1982, MNRAS, 199, 883
 Blandford R. D., & Znajek R. L., 1977, MNRAS, 179, 433
 Bloom J. S. et al, 2006, ApJ, 638, 354
 Eichler D., Livio M., Piran T., & Schramm D.N., 1989, Nature, 340, 126
 Fan Y.Z., Zhang B. & Proga D., 2005, ApJ, 635, L129
 Fryer C. L., & Woosley S. E., 1998, ApJ, 502, L9
 Galama T. J., 1998, Nature, 395, 670
 Gehrels N. et al. 2005, Nature, 437, 851
 Ghosh P., & Abramowicz M. A., 1997, MNRAS, 292, 887
 Gu W. M, Liu T., & Lu, J. F, 2006, ApJ, 643, L87
 Hjorth J., et.al., 2003, Nature, 423, 847
 Lee H. K., Wijers R. A. M. J., & Brown G. E., 2000, PhR, 325, 83
 Livio M., Ogilvie G. I., & Pringle J. E., 1999, ApJ, 512, 100
 Katz J. I., 1997, ApJ, 490, 233
 Kouveliotou C., et al., 1993, ApJ, 413, L101
 Narayan R., Piran T., & Kumar P., 2001, ApJ, 557, 949 (NPK)

- Narayan R., Paczynski B., & Piran T., 1992, ApJ, 395, L83
Narayan R., & Yi I., 1994, ApJ, 428, L13
Matteo T. D., Perna R., & Narayan R., 2002, ApJ, 579, 706 (DPN)
Mizuno Y. et al. 2004a, ApJ, 606, 395; 2004b, ApJ, 615, 389
Merloni A., & Fabian A. C., 2002, MNRAS, 332, 165
Meszaros P., & Rees M.J., 1997, ApJ, 482, L29
Paczynski B., 1998, ApJ, 494, L45
Perna R. Armitage P. & Zhang B. 2006, ApJ, 636 , L29
Proga D. et al. 2003, ApJ, 599, L5
Proga D. & Begelman M.C. 2003, ApJ, 592, 767
Proga D. & Zhang B., 2006, MNRAS, 370, L61
Popham R., Woosley S. E. & Fryer C., 1999, ApJ, 518, 356 (PWF)
Prian T., 1978, ApJ, 221, 652
Pringle J. E., 1981, ARA&A, 19, 137
Pudritz R. E., & Fahlman G.G, 1982, MNRAS, 198, 689
Shakura N. I., & Sunyaev R.A., 1973, A&A, 24, 337
Shibata M. et al., 2006, PRL , 96, 031102
Stanek K. Z., et.al., 2003, ApJ, 591, L17
Toomre A., 1964, ApJ, 139, 1217
Torkelsson U., Brandenburg A., Nordlund A., & Stein R. F., 1996, ALC, 34, 383
Usov V. V., 1992, Nature, 357, 472
Woosley S. E., 1993, ApJ, 405, 273
Zhang B., 2007, ChJAA, 7, 1